Spectrum - The Journal of Operational Applications in Defense Areas

Journal homepage: https://spectrum.ita.br

Electronic Warfare and Remote Sensing: Analysis and Prediction of Military Target Signatures

Electromagnetic Interference Between Naval Employment Radars

Newton A. S. Gomes[1], Mário D. A. Tavares[2], Renan M. Richter[1] and André P. Gonçalves[1]

[1]Aeronautics Institute of Technology - ITA, São José dos Campos/SP - Brazil

[2]Navy Weapons Systems Directorate - DSAM, Rio de Janeiro/RJ - Brazil

Article Info

Article History:

Received	15 May 2025
Revised	26 June 2025
Accepted	14 July 2025
Available online	23 September 2025

Keywords:

Interference
RCS
Radar Detection

E-mail adresses:

newtonsg@ita.br
tavares.diego@marinha.mil.br
richter@ita.br
andre.paim@marinha.mil.br

Abstract

The use of radars in the maritime environment has both civil and military applications. The effect of co-channel interference between radars deployed on different ships occurs frequently in several navies. This work proposes to develop a methodology to mitigate the effect of interference between radars operating at the same frequency. A hypothetical radar is used to simulate the effect of co-channel interference between ships, varying the azimuthal engagement angle and the distance between the ships. In the end, a topology of arrangement of ships in a column is obtained, with a maximum distance of 5.95 NM and an arrangement in line with a maximum value of 37.01 NM. This work shows that interference occurs between radars, being overly dependent on the angular condition of engagement due to the effect of the RCS (Radar Cross Section) of the interfering ship.

I. INTRODUCTION

Modern warfare has led to the deployment of several electronic systems in a naval environment. In an electronic warfare scenario, one of the elements of these systems is the radar, which represents one of the fundamental sensors for naval use.

Naval radar has the functions of navigation, early warning, and weapons control, for example, detecting and identifying targets in real time in various types of missions.

During their maritime movements, military ships form a standardized formation as shown in Fig. 1. However, the threat of mutual interference between radar systems is increasing as the military frequency range is expanded, as new communication/detection systems are implemented in the same frequency band or when new and old radars operate simultaneously in the same movement formation [1].

From this condition, interference protection procedures are necessary to avoid the degradation of radar systems in the combat operational radius. Due to this problem, this work proposes to develop a methodology to reduce the effect of co-channel interference between radars operating on the same frequency in a tactical formation.

To achieve this objective, the theoretical basis is presented in section II, describing the radar equation, the concept of RCS (*Radar Cross Section*), and the theory of radar detection and interference. Section III describes the use of a hypothetical radar, the development of the modeling and simulation of a ship, and the radar engagement planning. Section IV presents the RCS of a ship and the interfering effects on the signal-to-noise ratio in the detection process. Finally, the conclusion of this work is presented.

Fig. 1. Formation of ships from eight countries during the RIMPAC exercise in 2006 [2].

II. THEORETICAL FOUNDATIONS

A. Radar Equation and RCS

The concept of radar is associated with the propagation of electromagnetic waves developed from the studies of the

German physicist Heinrich Rudolf Hertz in 1883, where he applied the classical electrodynamics of Maxwell's equations [3].

Taking a pulse-doppler radar as a reference, its operating principle corresponds to the detection of the energy flux scattered by the target, measured in W/m^2, from the propagated electromagnetic waves [4]. The radar receiver detects and estimates the maximum distance between this target and the radar by (1) [5].

$$R_{max} = \sqrt[4]{\frac{P_t G^2 \lambda^2 \sigma}{(4\pi)^3 k_B T_e B W F_n (SNR_o)_{min}}} \tag{1}$$

As described in (1), the maximum radar range is conditioned by the receiver signal-to-noise ratio SNR_o, and is presented in more detail in the subsection B. The other terms in (1) are the transmitter power amplifier P_t, the antenna gain G, the emitted electromagnetic wavelength λ as a function of the operating frequency, the Boltzmann constant k_B, the system operating temperature T_e, the radar receiver bandwidth BW, the receiver noise figure F_n and σ which corresponds to the target's RCS, this being the only variable that does not depend on the radar system [6].

The RCS (σ) represents the ratio between the electric field scattered by the target $\vec{E}_s$ and the electric field incident on the radar $\vec{E}_i$ as a function of the azimuthal ϕ and elevation θ angles, (2), whose values are independent of the distance between the radar and the selected target [6].

$$\sigma(\theta, \phi) = \lim_{r \to \infty} 4\pi r^2 \frac{\left|\vec{E}_s(r, \theta, \phi)\right|^2}{\left|\vec{E}_i(r, \theta, \phi)\right|^2} \tag{2}$$

The RCS value in (2) is presented in m^2, and the value in $dBsm$, defined by (3), is also used. Due to the wide dynamic range of results to be obtained, RCS values are normally described in units of $dBsm$. This work uses RCS values in $dBsm$ [6].

$$\sigma = 10 \cdot \log_{10}(\sigma\,[m^2]) \;\; [dBsm] \tag{3}$$

In the naval field, determining the RCS of a ship is a major challenge. However, in 1978, experimental studies were carried out to measure the RCS of maritime targets [7]. Obtaining these values as a function of frequency and azimuths is essential for applying the radar equation to detect the ship under study. Table I describes the RCS values of some types of ships.

Table I. RCS values of typical ships [7].

Type	Dimension [m]	RCS [dBsm]
Coal Ship	73.45	30.5 ± 3.5
Frigate	103.02	44.5 ± 5.5
Container Ship	211.83	44.0 ± 4.0

B. Radar Detection

In a radar system, the receiver has the function of detecting the target. This condition is obtained when the echo signal S, measured in watts, in relation to the noise N, also measured in watts, has a value capable of discriminating the radar reflection signal from the system noise. The relationship between the signal and the noise is called SNR (*Signal-to-Noise Ratio*), determined in dB (decibels). The radar receiver in use has a constant SNR_0, which defines the minimum target detection ratio, named $SNR_{0(min)}$, and described in Fig. 2 [8].

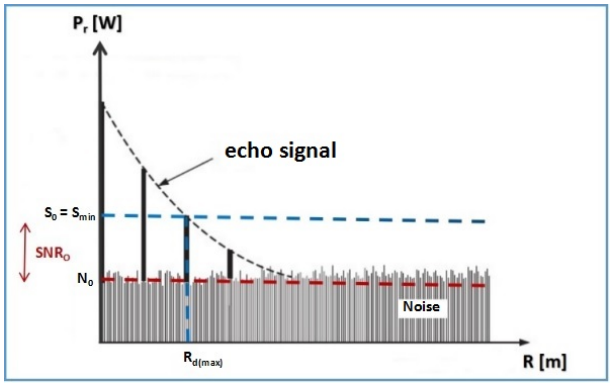

Fig. 2. Description of radar detection of a target as a function of the power received by a receiver determining the maximum range [8].

In this context, for radar detection to occur, the relation (4) must be met, with N_0 being the noise floor of the radar receiver. According to Fig. 2, when S corresponds to a value S_{min}, the maximum target detection distance $R_{d(max)}$ is determined.

$$S \geq SNR_{0(min)} + N_0 \tag{4}$$

Another way of presenting the detection condition is to evaluate, temporally, the signal-to-noise ratio SNR received by the receiver in relation to the minimum detection condition of the radar receiver in use, summarized in (5).

$$SNR \geq SNR_{0(min)} \tag{5}$$

C. Radar Interference

Electromagnetic interference is intended to make it impossible for a communication and/or detection system to use the electromagnetic spectrum in a given frequency band for a given period of time.

According to Fig. 3, a diagram of signals as a function of time acting on the radar receiver is presented.

The interference signal I is inserted into the radar receiver, changing the detection condition described in (5), since with the inclusion of the interference I, the noise ceiling N_0 rises. The detection condition is now determined by (6).

$$\left(\frac{S_0}{N_0 + I}\right) \geq SNR_{0(min)} \tag{6}$$

When it comes to performing interference between radars, there are three possible conditions for its execution. The first condition is mutual coupling; the second possibility is when the sensitivity is common between the receivers, which is related to the transmission signal and signal processing used; and, finally, the distance between the radar systems [9].

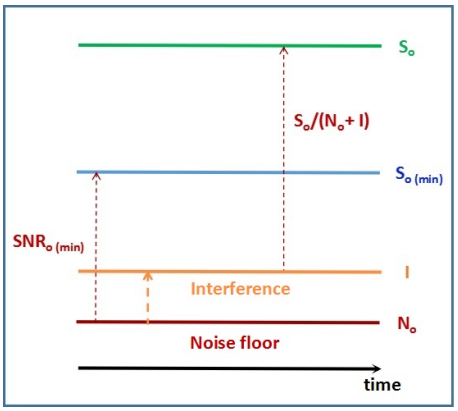

Fig. 3. Diagram of signals as a function of time in the radar receiver.

III. MATERIALS AND METHODS

A. Hypothetical Radar

This work uses the concept of a hypothetical radar to evaluate the technical requirements of a general-purpose naval radar. The data are presented in Table II.

Table II. Technical data of the hypothetical radar.

Operating Frequency	9.41 GHz	PW	600 ns
Rotation Speed	12 RPM	PRI	2.5 ms
Antenna Vertical Aperture	50°	AMNA	202 NM
Polarization	Horizontal	Peak Power	20 kW
P_{fa}	10^{-6}	G	32 dB

Radars can determine a maximum range, defined by the acronym AMNA (*Maximum Unambiguous Range*). For the hypothetical radar used in this work, it is worth 202 NM (374.1 km). The AMNA is correlated with the PRI (*Pulse Repetition Interval*), which represents the emission rate of a radar pulse [10].

There is also a minimum distance at which the radar begins its detection, defined by the pulse width (PW) of the electromagnetic wave emitted by the transmitter. In the case of the hypothetical radar, it is a value close to 0.048 NM (90 m) [10].

The $SNR_{0(min)}$ of the hypothetical radar is set to a value of 31.73 dB at the radar's operating frequency. Considering a temperature T_e of 313 K, a BW of 60 MHz, and a F_n of 4.7 dB, the noise ceiling N_0 is obtained at -118.7 dBW. Using (4), the condition for detection to occur in the hypothetical radar, without interference, is that $S \geq -86.97$ dBW.

B. Ship Modeling and Simulation

In this study, a CAD (*Computer Aided Design*) of a ship with geometric characteristics equivalent to those used in navies is used, on a scale 1 : 1, which implies obtaining a high correlation to the real environment, Fig. 4.

The software used in the study is FEKO®, from ALTAIR, and the asymptotic RL-GO (*Ray Launching - Geometrical Optics*) method is applied with discretizations (*mesh*) of $\lambda/10$ in CAD. All modeling and simulations were performed on an Intel Xeon E-2246 machine with 12 cores and 64 GB RAM.

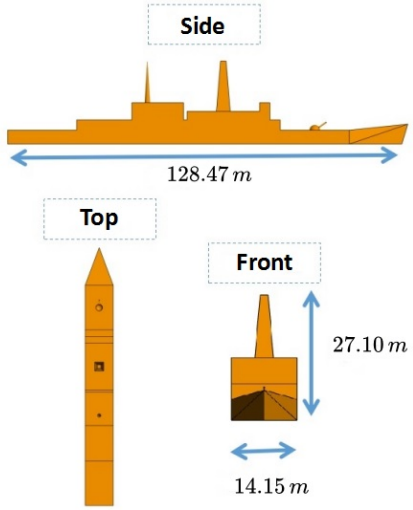

Fig. 4. Ship geometry used in electromagnetic simulations.

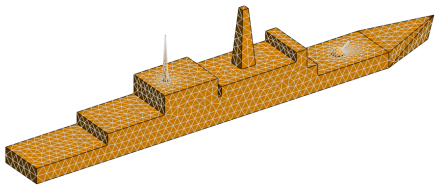

Fig. 5. Presentation of the *mesh* modeled in FEKO® for the ship.

The material used in the CAD model is metallic (PEC - *Perfect Electric Conductor*). The *mesh* performed in FEKO® obtained a structure with a total of $3,318$ triangles with edges of dimensions worth 1.98 ± 0.72 m, having a maximum of 3.63 m and a minimum of 0.06 m, Fig. 5.

C. Engagement Planning

Figure 6 shows the radar engagement arrangement in 360° of azimuth ϕ, with the angle 0° being the stern, 90° being the starboard beam, 180° being the bow, and 270° being the port beam.

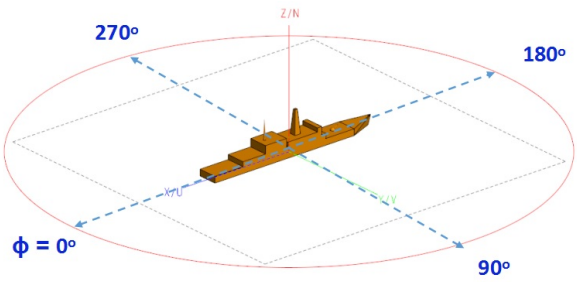

Fig. 6. Overview of the engagement angles performed by the radar on the ship.

The hypothetical radar is simulated at a frequency of 9.41 GHz in horizontal polarization. The methodology employed

consists of performing engagement at all azimuthal angles with steps of $1°$.

The experiment carried out corresponds to understanding the positioning condition of a victim ship in relation to the interfering ship, which receives the effect of the interference, and the interfering ship, which carries out the interference, varying the azimuth ϕ and the distance R according to the topological arrangement described in Fig. 7. The victim and interfering ships perform a displacement in parallel displacement trajectories.

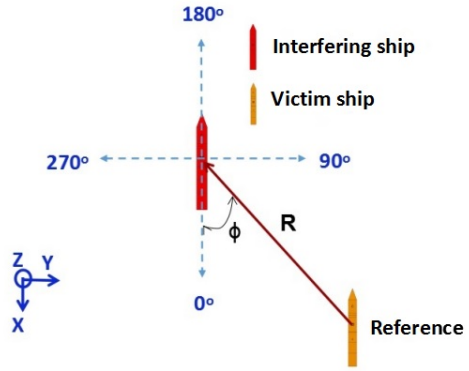

Fig. 7. Top view of the engagement procedure between the victim and the interfering ship with a distance R and azimuth ϕ.

Four hypothetical conditions are used to perform this analysis. The first condition is that the antennas are synchronized in a condition in which the main lobes of the radar antennas are in phase opposition at maximum gain, as shown in Fig. 8. A second condition is that the temporal diagrams of the radar pulses are in phase, with the same pulse width (PW) and the same pulse repetition interval (PRI). The third condition is that the sea is calm, with no *clutter* originating from sea waves. The fourth condition is that the engagements are performed one-to-one, with no third or more ships in the process. These ideal propositions correspond to a hypothesis of maximum possibility of interference, being a worst-case condition to be analyzed for the victim ship.

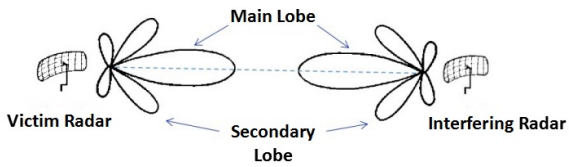

Fig. 8. Diagram of engagements between the victim radar and the interfering radar.

IV. RESULTS AND DISCUSSION

A. Ship Static RCS

Applying the ship's CAD in FEKO®, the modeling of the Poynting vector emission $\vec{S}$ is performed as shown in Fig. 9, having an azimuthal variation of $0° \leq \phi < 360°$ and an elevation of $\theta = 90°$.

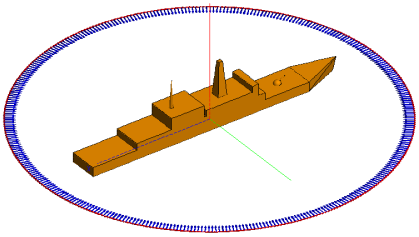

Fig. 9. CAD modeling of the ship to determine the static RCS.

In Fig. 10 the RCS values, in dBsm, as a function of the azimuth ϕ are presented. The time taken to determine the RCS was 2 days, 10 hours, and 3 minutes. From the data obtained, it is observed that the highest values are in the azimuths of $0°$, $90°$, $180°$, and $270°$, with an average RCS of 25.29 ± 10.82 dBsm having a maximum value of 100.07 dBsm and a minimum value of -0.30 dBsm.

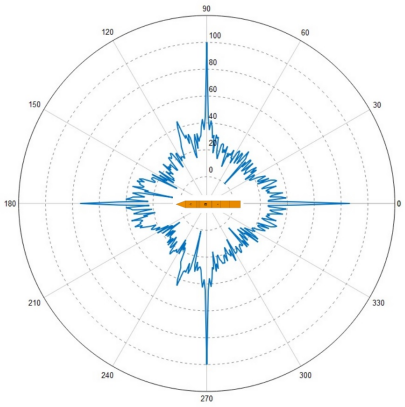

Fig. 10. Static RCS of the ship, in polar form, with radial axis in dBsm.

From the data obtained from the ship's RCS, the values of S_0 are determined as a function of ϕ with steps of $1°$.

B. Signal-to-Noise Ratio of Ship Interference

Considering the hypothetical radar data, the effect of the distance between the interfering signal source and the victim of the interference changes the signal diagram presented in Fig. 3. Referring to the equation (1), the detection distance R is related to the condition $R \sim \sqrt[4]{1/SNR}$. Considering the case in which the interference $I = 0$, the increase in the distance R between the ships, at a fixed azimuth ϕ, corresponds to a lower value of SNR. By employing the hypothetical radar data, the minimum range marking, the AMNA, the noise ceiling N_0, and the radar echo signal S_0 are plotted, Fig. 11.

When engaging a ship that has an RCS of $4\,m^2$ at a given azimuth ϕ, the maximum detection range R_d without interference is 26.94 NM. At this distance, which corresponds to the maximum range, the receiver has an $SNR = SNR_{0(min)} = 31.73$ dB. From this point on, the radar loses detection of the target, and the value of SNR decreases until $S_0 = N_0$, described in (4). This condition corresponds to the *crossover* distance R_{co}, which represents the condition

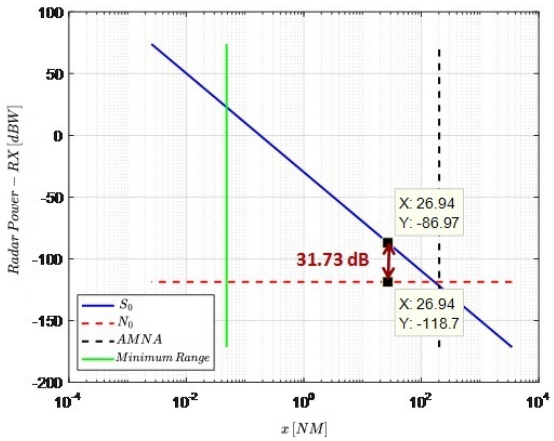

Fig. 11. Diagram of signals as a function of the distance between the victim and interfering ship when $I = 0$, identifying the *crossover* point (R_{co}).

in which the radar echo signal is equal to the noise ceiling. From this distance on, the noise signal N_0 is greater than the radar echo signal S_0, providing a natural interference condition in the radar system.

Figure 12 shows the value of R_d applied to the RCS data obtained in the ship simulation as a function of the azimuths ϕ, where d_{max} corresponds to the AMNA value and d_{min} represents the minimum distance detectable by the hypothetical radar. In all calculated azimuths, the *crossover* distance R_{co} is above the AMNA value.

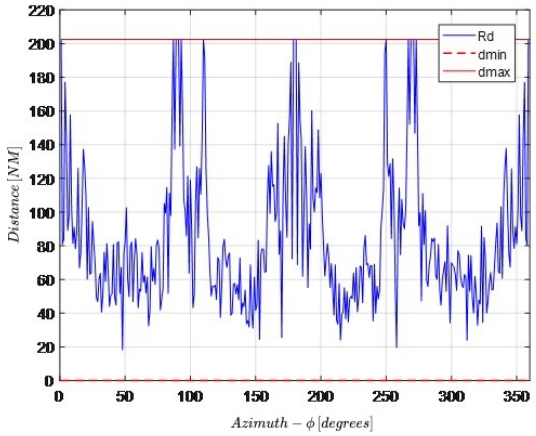

Fig. 12. Detection range R_d of the interfering ship by the victim ship when $I = 0$.

When evaluating the data in Fig. 12, in all engaged azimuths, the interfering ship is detected, having a minimum range value of 18.23 NM (33.76 km) and a maximum value of 202.48 NM (375.00 km). It is important to note that outside the azimuths of 0°, 90°, 180°, and 270°, the RCS drops abruptly to values around 20 dBsm ($100\,m^2$), which leads to a significant decrease in the detection range in diagonal radar engagement conditions.

At the moment the interfering ship activates its radar, the noise ceiling rises, being determined by $N_0 + I$. Considering the previous engagement condition with the angle ϕ, with the RCS of $4\,m^2$, the radar range with interference R_{dI} is smaller than the minimum range of the hypothetical radar, and the *crossover* distance with interference R_{coI} is worth 0.086 NM (159.27 m), Fig. 13.

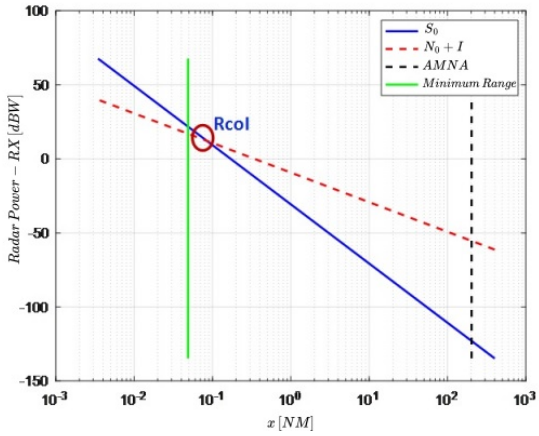

Fig. 13. Signal diagram as a function of distance between the victim and interfering ship when $I > 0$, identifying the interference *crossover* point (R_{coI}).

The value of R_{coI}, Fig. 13, corresponds to the position in relation to the victim ship in which the interfering ship stops interfering, but without its detection by the victim ship. In summary, if the physical distance R, Fig. 7, between the victim ship and the interfering ship is greater than R_{coI}, the interference is effective on the victim ship.

Based on this analysis, the value of R_{coI} is calculated in all engagement azimuths and presented in Fig. 14.

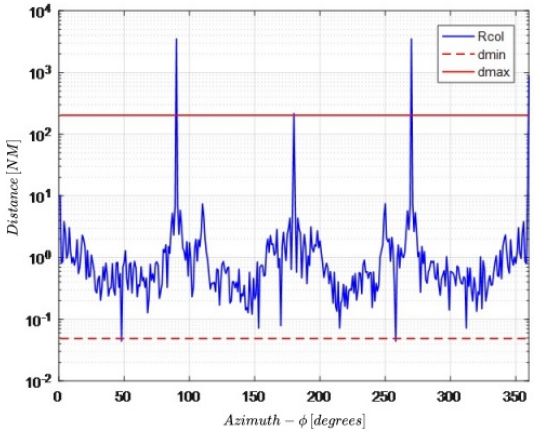

Fig. 14. Arrangement of R_{coI} values in relation to the engagement azimuths ϕ of the victim ship.

According to Fig. 14, the values of R_{coI} have a high variation as a function of the azimuth ϕ. In order to avoid the effect of interference between radars in a naval formation at any azimuthal angle, the condition of lowest R_{coI} is chosen, having a value of 0.13 NM (240.76 m).

However, there are angles ϕ at which the values of R_{coI} are very high, Fig. 14. At angles of 0°, 90°, 180°, and 270°, R_{coI} is at the detection limit of the hypothetical radar of

202 NM (374.1 km), which allows navigation with the ships when arranged in a line or column.

Even with high values of R_{coI} in these azimuths, the value of R_{dI} is calculated, which corresponds to the maximum detection range of the interfering ship by the victim ship with effective interference. These values are presented in Table III.

Table III. Values of R_{dI} for specific azimuths.

Azimuth [degrees]	RCS [dBsm]	R_{dI} [NM]
0°	86.43	24.28
90°	100.07	37.01
180°	74.21	5.95
270°	100.07	37.01

According to Fig. 15, in the condition of ships in column, the probable angles are 0° or 180°. The lowest value of R_{dI} is recommended. In this case, the distance between ships in column d_c should be less than 5.95 NM (11.02 km). In the condition of ships in line, the probable angles are 90° or 270°. In this case, it is recommended that the distance between ships in line d_l should be less than 37.01 NM (68.54 km).

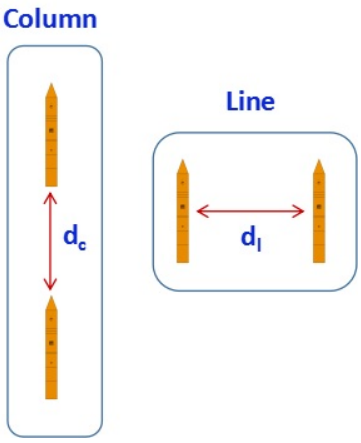

Fig. 15. Arrangement of formation in line and column.

V. CONCLUSION

This work aims to understand the behavior of the electromagnetic effect of two naval radars operated on different ships, at the same frequency and in different azimuth conditions. The concept of a hypothetical radar is used to perform the set of technical analyses.

Through electromagnetic simulations of the ship, RCS values were calculated as a function of the engagement azimuths. From these values, SNR ratios were obtained for conditions with and without interference. It is evident that interference occurs between radars, being highly dependent on the angular condition of engagement due to the effect of the RCS of the interfering ship.

The interference effect is less effective at angles of 0°, 90°, 180°, and 270°. Based on this condition, a maritime formation arrangement is suggested in order to mitigate the interference effect when all ships use the same radar with equal frequencies, with column and line formation being ideal for this situation.

This study contributes, in a technical way, to the understanding of the effect of co-channel interference between naval radars, proposing arrangements and distances between ships aimed at mitigating the effects of these interferences, on operational movements.

VI. ACKNOWLEDGEMENTS

The authors thank the company ALTAIR for providing access to the FEKO® software throughout the electromagnetic modeling and simulation process.

REFERENCES

[1] H. Kim, Y. Kim, M. Kang, S. Cho, and B. Kim, "Inter-Radar Interference Analysis Based on L and S Band Propagation Models and Radar Beam-Scanning Scenarios," *IEEE Access*, vol. 10, pp. 125 744–125 753, 2022.

[2] Seaman James R. Evans, "Rimpac battlegroup 2006," Available at: https://commons.wikimedia.org/w/index.php?curid=2213083. Accessed on: July 22, 2024.

[3] D. J. Griffiths, *Eletrodinâmica*, 3rd ed. São Paulo: Pearson Addison Wesley, 2011.

[4] C. Balanis, *Teoria de Antenas*. Rio de Janeiro: LTC, 2009, vol. 1.

[5] B. Mahafza, *Radar Signal Analisys and Processing using Matlab*, Alabama, 2009.

[6] E. F. Knott, J. F. Schaeffer, and M. T. Tulley, *Radar Cross Section*. SciTech Publishing, 2004.

[7] P. Williams, H. Cramp, and K. Curtis, "Experimental Study of the Radar Cross-Section of Maritime Targets," *IEE Journal on Electronic Circuits and Systems*, vol. 2, no. 4, pp. 121–136, 1978.

[8] G. W. Stimson, *Instroduction to Airborne Radar*, 2nd ed. Mendham: SciTech Publishing, 1998.

[9] O. van Gent, R. van Heijster, M. Heiligers, A. Theil, M. Driesse, and W. Sahebali, "TNO 2020 R11396 - Radar Interference Study," 2021.

[10] M. I. Skolnik, *Introduction to Radar Systems*. McGraw-Hill, 1980.